

## Coherent propagation of polaritons in semiconductor heterostructures: Nonlinear pulse transmission in theory and experiment

S. Schumacher, G. Czycholl, and F. Jahnke

*Institute for Theoretical Physics, University of Bremen, 28334 Bremen, Germany*

I. Kudyk, L. Wischmeier, I. Rückmann, T. Voss, and J. Gutowski

*Institute for Solid State Physics, Semiconductor Optics Group, University of Bremen, 28334 Bremen, Germany*

A. Gust and D. Hommel

*Institute for Solid State Physics, Semiconductor Epitaxy Group, University of Bremen, 28334 Bremen, Germany*

(Received 22 June 2005; published 23 August 2005)

The influence of coherent optical nonlinearities on polariton effects is studied by means of a detailed comparison of theory and experiment. A unique approach that combines a microscopic treatment of the boundary problem in a sample of finite thickness with excitonic and biexcitonic nonlinearities is introduced. Spectral changes that depend on the light polarization are analyzed for single pulse transmission and pump and probe excitation.

DOI: [10.1103/PhysRevB.72.081308](https://doi.org/10.1103/PhysRevB.72.081308)

PACS number(s): 71.36.+c, 71.35.Cc

The propagation of light pulses which are coupled to the excitonic resonances is a fundamental problem in semiconductor optics that has been the subject of intense experimental and theoretical research. The observations are dominated by the strong light-matter interaction and its interplay with the inherent many-particle Coulomb interaction of the electronic system. In the linear optical regime, exciton polaritons give rise to effects such as polariton beating in the time-resolved pulse transmission<sup>1</sup> or yield strong modifications of excitonic transmission spectra, see, e.g., Refs. 2–4. In the nonlinear optical regime, incoherent saturation of the polariton resonances in transmission spectra<sup>5,6</sup> and in the amplitude and phase of the time-resolved transmission,<sup>7</sup> as well as transmission changes in pump and probe experiments,<sup>8</sup> have been studied.

The above investigations are focused on samples where the thickness corresponds to a few exciton Bohr radii where polariton effects are most pronounced in the optical spectra. In this case the interplay of the induced excitonic polarization in the medium with the propagating light field is strongly influenced by sample surfaces which considerably complicates the theoretical description. In a frequently used phenomenological approach<sup>9</sup> the coupling of the exciton relative and center-of-mass (COM) motion at the sample boundaries is neglected. Then, the exciton COM motion is subject to quantization effects in the confinement geometry while the exciton relative motion is approximated by the result of the infinitely extended medium. As a result of this approach, the solution of the wave equation for the electromagnetic field requires additional boundary conditions (ABCs) (Refs. 9 and 10) which are, however, not uniquely defined. Unfortunately, in many situations the choice of ABCs can influence the theoretical predictions.<sup>11</sup> To avoid these ambiguities, the use of microscopic boundary conditions within a *nonlocal* semiconductor response has been discussed in Ref. 12 and recently applied to the linear optical regime.<sup>3,4,13</sup> The description of optical nonlinearities com-

bined with a microscopic treatment of boundary conditions has been restricted so far to the quantum-well (QW) limit where propagation effects lead to radiative exciton broadening, which can be modified in radiatively coupled QWs. Furthermore, excitonic nonlinearities in QWs have been studied in connection with microcavity polaritons; for a review, see Ref. 14. In the opposite limit of the sample thickness approaching the bulk limit, nonlinear pulse propagation effects<sup>15,16</sup> have been analyzed successfully within a local approach for the semiconductor response. The decoupling of relative and COM exciton motion has also been used in an earlier approach to study the influence of propagation effects on four-wave mixing signals.<sup>17</sup>

In this paper we present a unique approach that describes the combined influence of polariton propagation effects and coherent excitonic and biexcitonic nonlinearities. While the theoretical understanding of the coherent nonlinear excitation dynamics in QW or bulk systems is well developed, the additional influence of propagation effects is missing, especially in a regime where the sample thickness exceeds the QW limit but the heterostructure interfaces prevent bulklike behavior. In this case, typically, several well-resolved polariton modes contribute to the optical properties and, as is shown by our investigations, the Coulomb interaction of the corresponding excitonic states modifies optical nonlinearities.

Our approach is based on a direct solution of the two- and four-particle Schrödinger equations for the exciton and biexciton motion together with Maxwell's equations. We apply microscopic boundary conditions to avoid ambiguities due to ABCs in situations where both material polarization and optical fields are strongly influenced by the boundaries of the system. A direct comparison of nonlinear transmission spectra for a ZnSe/ZnSSe heterostructure shows excellent agreement between theory and experiment, and supports the detailed analysis of the microscopic model. As another application, calculated pump and probe spectra for a GaAs/AlGaAs heterostructure are presented.

In the coherent regime, excitonic and biexcitonic nonlinearities up to third order in the optical field can be consistently described in terms of the dynamics-controlled truncation (DCT) formalism,<sup>18,19</sup> which has been successfully applied in the past to QW systems.<sup>20–25</sup> We extend this formalism to layers with a finite thickness where the sample boundaries still provide a confinement potential for the electrons and holes. To account for the coupling of the exciton relative and COM motion, independent coordinates for the electron and hole motion in propagation direction are used while these carriers are subject to Coulomb interaction (treated on the level of DCT) and to the optical field.

We consider a two-band model with spin-degenerate conduction and valence bands to describe the spectrally lowest interband transitions for a semiconductor layer in a slab geometry<sup>11</sup> with strain-split light- and heavy-hole valence bands. The resonant contribution to the spatially inhomogeneous polarization in the semiconductor,

$$\mathbf{P}(z, t) = d_{eh}^* \sum_{\mathbf{k}} (p_{(\mathbf{k}, z, z)}^{(-1/2)(-3/2)} \mathbf{e}_+ + p_{(\mathbf{k}, z, z)}^{(+1/2)(+3/2)} \mathbf{e}_-), \quad (1)$$

is given in terms of the *nonlocal* excitonic transition amplitude  $p_{(\mathbf{k}, z_e, z_h)}^{eh}(t) = \langle h_{\mathbf{k}}(z_h) e_{\mathbf{k}}(z_e) \rangle$  with the electron  $e_{\mathbf{k}}(z_e)$  and hole  $h_{\mathbf{k}}(z_h)$  operators, respectively. According to the dipole selection rules, the  $(-\frac{1}{2}, -\frac{3}{2})$  and  $(+\frac{1}{2}, +\frac{3}{2})$  transitions are independently driven by circular optical polarization with unit vectors  $\mathbf{e}_+$  and  $\mathbf{e}_-$ , respectively,  $\mathbf{k}$  is the in-plane carrier momentum (for the directions possessing translational invariance) and  $e, h$  are quantum numbers that simultaneously denote the band index and the  $z$  component of the corresponding total angular momenta. A local dipole interaction  $\mathbf{d}_{eh}(\mathbf{k}, z_e - z_h) = \mathbf{d}_{eh} \delta(z_e - z_h)$  is used. Applying the DCT scheme, an equation of motion for the excitonic transition amplitude  $p_{(\mathbf{k}, z_e, z_h)}^{eh}$  is obtained, which is coupled to the biexcitonic correlation function,

$$\begin{aligned} b_{eh}^{e'h'}(\mathbf{k}_2, z_2, \mathbf{k}_1, z_1) &= \langle h'_{\mathbf{k}_1}(z_1) e'_{\mathbf{k}_2}(z_2) h_{\mathbf{k}_3}(z_3) e_{\mathbf{k}_4}(z_4) \rangle \\ &\quad - \langle h'_{\mathbf{k}_1}(z_1) e'_{\mathbf{k}_2}(z_2) \rangle \langle h_{\mathbf{k}_3}(z_3) e_{\mathbf{k}_4}(z_4) \rangle \\ &\quad + \langle h'_{\mathbf{k}_1}(z_1) e_{\mathbf{k}_4}(z_4) \rangle \langle h_{\mathbf{k}_3}(z_3) e'_{\mathbf{k}_2}(z_2) \rangle, \end{aligned} \quad (2)$$

that itself obeys a four-particle Schrödinger equation with coherent source terms.<sup>26</sup> The resulting closed set of equations contains all mean-field (Hartree-Fock) as well as biexcitonic contributions to the semiconductor response up to third order in the optical field. The evaluation of these material equations is performed in the exciton eigenbasis. As an important ingredient of our approach, exciton eigenfunctions  $\phi_m(\mathbf{k}, z_e, z_h)$  are determined for the given confinement geometry to include the additional nonlocal space dependence. In contrast to Ref. 13 we use eigenfunctions that individually fulfill the boundary conditions of the system.<sup>4,27</sup> Then every eigenfunction corresponds to a polariton resonance in the linear optical spectrum and a truncation of the expansion can be justified with the considered spectral range while the boundary conditions of the inhomogeneous system remain fully satisfied. The excitonic transition amplitude and the sin-

glet ( $\lambda = -1$ ) and triplet ( $\lambda = +1$ ) contributions to the biexcitonic correlation function are expressed as

$$P_{(\mathbf{k}, z_e, z_h)}^{eh}(t) = \sum_m P_m^{eh}(t) \phi_m(\mathbf{k}, z_e, z_h), \quad (3)$$

$$\begin{aligned} b_{eh}^{e'h'}(\mathbf{k}_2, z_2, \mathbf{k}_1, z_1) &= \sum_{nm} [\phi_n(\alpha \mathbf{k}_4 + \beta \mathbf{k}_3, z_4, z_3) \phi_m(\alpha \mathbf{k}_2 \\ &\quad + \beta \mathbf{k}_1, z_2, z_1) \times b_{nm}^{eh'e'h'}(\mathbf{k}_4 - \mathbf{k}_3, t) \\ &\quad - \lambda \phi_n(\alpha \mathbf{k}_2 + \beta \mathbf{k}_3, z_2, z_3) \phi_m(\alpha \mathbf{k}_4 \\ &\quad + \beta \mathbf{k}_1, z_4, z_1) \times b_{nm}^{eh'e'h'}(\mathbf{k}_2 - \mathbf{k}_3, t)], \end{aligned} \quad (4)$$

where  $p_m^{eh}(t)$  and  $b_{nm}^{eh'e'h'}(\mathbf{q}, t)$  are the time-dependent expansion coefficients.  $\alpha = m_h^*/M^*$  and  $\beta = m_e^*/M^*$  are the ratio of the hole and the electron masses to the total exciton mass  $M^* = m_e^* + m_h^*$ , respectively. This treatment generalizes the eigenfunction expansion in the QW limit discussed in Ref. 28. For a self-consistent description of the light propagation in a semiconductor material, Maxwell's equations are solved directly<sup>11</sup> together with the excitonic and the biexcitonic dynamics.

In Fig. 1 the theoretical and experimental results are shown for the transmission of a single light pulse through a high-quality 20-nm ZnSe layer sandwiched between two ZnSSe cladding layers. The sample was pseudomorphically grown by molecular-beam epitaxy on a (001)GaAs substrate. Further details on growth and sample characterization, as well as on modeling of the finite-height confinement potentials at the ZnSe/ZnSSe interfaces, are described in Ref. 4. The opaque GaAs substrate was carefully removed by grinding and subsequent chemical etching to permit measurements in transmission geometry. The sample was mounted onto a glass plate and kept on a cold finger in a microcryostat at a temperature of 4 K. A frequency doubled self-mode-locked Ti:sapphire laser with 110 fs full width at half maximum (FWHM) pulse duration and 83 MHz repetition rate was used as excitation source for the spectrally resolved but time-integrated transmission experiments. The maximum of the spectral pulse profile was set close to the spectral position of the first heavy-hole (hh1) polariton mode to excite the whole spectral region from the exciton-biexciton transition up to the hh2 and hh3 polariton resonances, as shown by the dotted line in Fig. 1(a). Linear or circular light polarization was selected using a Pockels cell. The transmitted signal was analyzed with a spectrometer and was recorded with a Charge-Coupled device (CCD) camera.

The measured linear transmission spectrum in the vicinity of the heavy-hole (hh) exciton resonance, depicted as a dashed-dotted line in Fig. 1(a), exhibits three pronounced polariton resonances denoted by hh1-hh3. With the microscopic treatment of boundary conditions, these polariton modes are perfectly reproduced in Fig. 1(c) (without adjustable parameters like a dead-layer thickness, the sample thickness has been independently determined using x-ray diffraction).<sup>4</sup> Results for nonlinear transmission spectra are shown in Figs. 1(a) (experiment) and 1(c) (theory) where

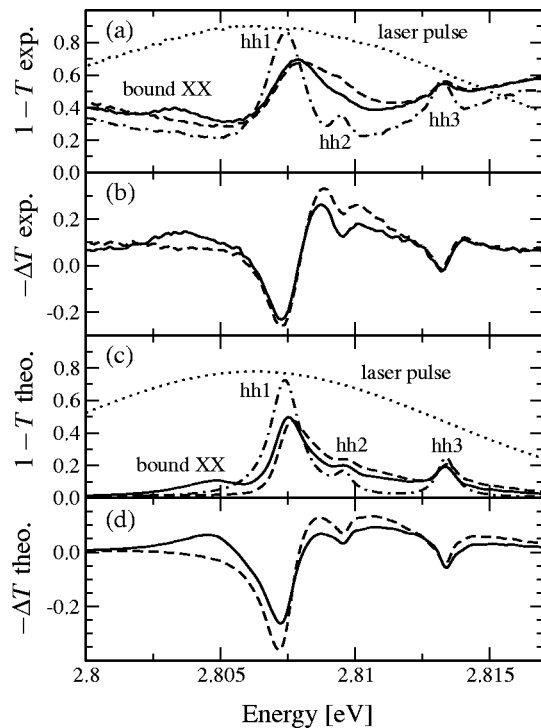


FIG. 1. (a) Dashed-dotted line: Linear transmission  $T$  (depicted as  $1-T$ ) for a pulse energy of 1.2 pJ for the 20-nm ZnSe sample. Dotted line: Spectral shape of the 110-fs laser pulse. Nonlinear transmission for a pulse energy of 12.2 pJ for linear (solid line) and circular (dashed line) light polarization. (b) Optically induced transmission changes  $\Delta T$  for linear (solid line) and circular (dashed line) light polarization, corresponding to the data in (a). (c) and (d) Theoretical results corresponding to (a) and (b), without the influence of Fabry-Perot effects (see discussion in the text).

linear and circular light polarization has been used. For better comparison, the optically induced transmission changes  $\Delta T = T_{\text{nonlinear}} - T_{\text{linear}}$  are given in Figs. 1(b) and 1(d), for the experiment and theory, respectively. The outermost surfaces between the cladding layer and air lead to a decreased transmission as well as to weak Fabry-Perot effects in the experiment.<sup>4</sup> In order to avoid additional parameters, the theory only includes intrinsic polariton effects. The constant offset in the measured nonlinear transmission results from slight intensity drifts of the applied laser pulses. These effects are of minor importance for the discussion here, since they just cause a nearly constant offset in the investigated transmission changes. The appearance of a bound biexciton (XX) resonance for linear optical polarization, which is absent for circular optical polarization according to its spin-singlet symmetry, is clearly identified in the theory-experiment comparison. The spectral changes at the polariton resonances result from mean-field (Hartree-Fock) as well as from biexcitonic correlations. For circular light polarization only the biexcitonic continuum states with electronic triplet configuration are excited, whereas for linear light polarization both singlet and triplet biexcitonic states contribute to the transmitted signal. In particular, an advantage of the theoretical approach applied here is the simultaneous inclusion of the bound biexciton state and the exciton-exciton scatter-

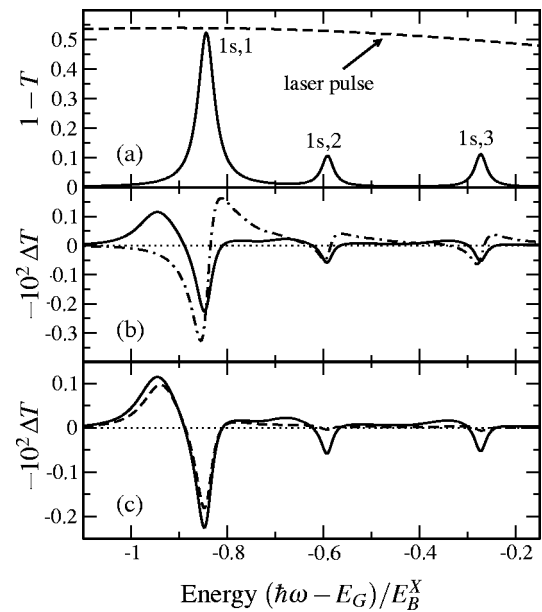


FIG. 2. (a) Solid line: Calculated linear transmission  $T$  (depicted as  $1-T$ ) for a GaAs layer with five exciton Bohr radii thickness. Dashed line: Spectral shape of a 120-fs laser pulse. (b) Differential probe transmission  $\Delta T$  for opposite circular (solid line), and cocircular (dashed-dotted line) polarization of pump and probe pulses. (c) Differential probe transmission  $\Delta T$  for opposite circular polarization including all Coulomb terms (solid line) and without Coulomb interaction of different polaritons (dashed line).

ing continuum. The latter is essential to reproduce the broad background on the high-energy side of the polariton resonances in the nonlinear transmission spectra. As a minor aspect, the biexciton binding energy is slightly underestimated by the truncation of the exciton basis, similar to the result in Ref. 25 for a QW system.

To provide further insight into the nature of coherent nonlinear polariton saturation, we also studied the pump and probe excitation for a GaAs layer embedded between AlGaAs barriers.<sup>29</sup> This part of the paper is intended to demonstrate the potential of our theory within another application and to stimulate further experiments for this material system. In a good approximation, the carriers in the GaAs layer are confined by infinitely high potential barriers in the  $z$  direction.<sup>11</sup> The solid line in Fig. 2(a) shows the linear optical transmission  $T$  through a GaAs layer of five exciton Bohr radii thickness. The energy  $\hbar\omega$  is given relative to the bulk band-gap energy  $E_G$  and normalized to the corresponding exciton binding energy  $E_B^X$ . For the chosen layer thickness, the confinement of carriers in the  $z$  direction yields three polariton resonances of the  $1s$  exciton in the displayed part of the spectrum which are labeled by consecutive numbers.

For the pump and probe excitation, two 120 fs laser pulses (from slightly different directions) without time delay are considered. The dashed line in Fig. 2(a) corresponds to the pulse spectrum. Figure 2(b) shows changes in the probe-pulse transmission that are induced by the pump pulse for opposite circular (solid line) and cocircular (dashed-dotted line) polarization of pump and probe pulses. The probe pulse

enters the excitonic polarization in linear order only. For the pump pulse a Rabi energy  $d_{eh}|\mathbf{E}_{\text{pump}}|=0.01E_B^X$  is used which ensures a consistent description within our  $\chi^{(3)}$  theory. The transmission changes around the higher ( $1s, 2$  and  $1s, 3$ ) polariton resonances in Fig. 2(b) are similar to those around the lowest one ( $1s, 1$ ) but with a decreased amplitude. A similar dependence on the light polarization has been reported for the differential probe absorption around the  $1s$  exciton resonance in a QW system.<sup>21</sup> For opposite-circular polarization, the pump-induced changes in the probe transmission are exclusively determined by biexcitonic correlations;<sup>21</sup> no mean-field effects contribute. This configuration is chosen for the analysis of the Coulomb interaction between polaritons in states with different spatial distribution. The dashed line in Fig. 2(c) shows the result where Coulomb interaction that couples different eigenfunctions in the two-exciton product basis of Eq. (4) is artificially switched off. We encounter only a slight change of the nonlinearities around the lowest polariton resonance ( $1s, 1$ ), whereas for higher peaks ( $1s, 2$  and  $1s, 3$ ) the influence of the pump pulse almost vanishes. Therefore, Coulomb interaction between exciton states with different spatial distribution (corresponding to different po-

lariton resonances) turns out to be the main source for transmission changes of higher polariton states.

In summary, a theory for the nonlinear polariton dynamics in semiconductor heterostructures has been presented which consistently includes (i) propagation effects with microscopic boundary conditions for the induced material polarization, as well as for the optical fields, and (ii) excitonic and biexcitonic coherent nonlinearities previously studied only in QWs or one-dimensional model systems. The application to nonlinear transmission spectra for a ZnSe/ZnSSe heterostructure shows excellent agreement between theory and experiment. The influence of light-polarization-dependent excitonic and biexcitonic nonlinearities has also been demonstrated for a pump and probe excitation of a GaAs heterostructure. Coulomb interaction of polariton states with different spatial distribution turns out to strongly influence the nonlinear optical transmission.

The authors acknowledge a grant for CPU time from the John von Neumann Institute for Computing at the Forschungszentrum Jülich. We thank G. Alexe for the sample characterization via x-ray diffraction.

<sup>1</sup>D. Fröhlich *et al.*, Phys. Rev. Lett. **67**, 2343 (1991).

<sup>2</sup>A. Tredicucci *et al.*, Phys. Rev. B **47**, 10348 (1993).

<sup>3</sup>J. Tignon *et al.*, Phys. Rev. Lett. **84**, 3382 (2000).

<sup>4</sup>S. Schumacher *et al.*, Phys. Rev. B **70**, 235340 (2004).

<sup>5</sup>U. Neukirch and K. Wundke, Phys. Rev. B **55**, 15408 (1997).

<sup>6</sup>M. Betz *et al.*, Phys. Rev. B **65**, 085314 (2002).

<sup>7</sup>J. S. Nägerl *et al.*, Phys. Rev. B **63**, 235202 (2001).

<sup>8</sup>A. C. Schaefer and D. G. Steel, Phys. Rev. Lett. **79**, 4870 (1997).

<sup>9</sup>S. I. Pekar, Sov. Phys. JETP **6**, 785 (1958).

<sup>10</sup>C. S. Ting, M. J. Frankel, and J. L. Birman, Solid State Commun. **17**, 1285 (1975).

<sup>11</sup>H. C. Schneider *et al.*, Phys. Rev. B **63**, 045202 (2001).

<sup>12</sup>A. D'Andrea and R. Del Sole, Phys. Rev. B **25**, 3714 (1982); A. D'Andrea and R. Del Sole, *ibid.* **41**, 1413 (1990).

<sup>13</sup>E. A. Muljarov and R. Zimmermann, Phys. Rev. B **66**, 235319 (2002).

<sup>14</sup>G. Khitrova *et al.*, Rev. Mod. Phys. **71**, 1591 (1999).

<sup>15</sup>H. Giessen *et al.*, Phys. Rev. Lett. **81**, 4260 (1998).

<sup>16</sup>J. Förstner, A. Knorr, and S. W. Koch, Phys. Rev. Lett. **86**, 476 (2001).

<sup>17</sup>A. Schulze, A. Knorr, and S. W. Koch, Phys. Rev. B **51**, 10601 (1995).

<sup>18</sup>V. M. Axt and A. Stahl, Z. Phys. B: Condens. Matter **93**, 195 (1994).

<sup>19</sup>M. Lindberg, Y. Z. Hu, R. Binder, and S. W. Koch, Phys. Rev. B **50**, 18060 (1994).

<sup>20</sup>V. M. Axt *et al.*, Z. Phys. B: Condens. Matter **188**, 447 (1995).

<sup>21</sup>C. Sieh *et al.*, Phys. Rev. Lett. **82**, 3112 (1999).

<sup>22</sup>W. Schäfer, R. Lövenich, N. A. Fromer, and D. S. Chemla, Phys. Rev. Lett. **86**, 344 (2001).

<sup>23</sup>N. H. Kwong *et al.*, Phys. Rev. B **64**, 045316 (2001).

<sup>24</sup>M. E. Donovan *et al.*, Phys. Rev. Lett. **87**, 237402 (2001).

<sup>25</sup>M. Buck *et al.*, Eur. Phys. J. B **42**, 175 (2004).

<sup>26</sup>W. Schäfer and M. Wegener, *Semiconductor Optics and Transport Phenomena* (Springer Berlin, 2002).

<sup>27</sup>S. Schumacher, G. Czycholl, and F. Jahnke, Phys. Status Solidi B **234**, 172 (2002).

<sup>28</sup>R. Takayama *et al.*, Eur. Phys. J. B **25**, 445 (2002).

<sup>29</sup>Material parameters are:  $m_e^*=0.067m_0$ ,  $m_h^*=0.457m_0$  for effective electron and hole masses, with the bare electron mass  $m_0$ , the background refractive index  $n_{\text{bg}}=3.71$ , a dephasing constant  $\gamma=0.06$  meV, the bulk GaAs band-gap energy  $E_G=1.42$  eV, and a dipole coupling constant  $d_{eh}/e_0=5$  Å.